




**Polarization conversion in the caviton driven by linearly polarized lasers**S. T. Zhang <sup>1</sup>, T. Yang,<sup>2</sup> Y. Z. Zhou,<sup>1</sup> Y. Jiang <sup>1</sup>, R. Xie,<sup>1</sup> D. J. Liu <sup>2</sup>, X. M. Li,<sup>2</sup> B. Qiao,<sup>1</sup> Z. J. Liu,<sup>1,2,\*</sup> L. H. Cao,<sup>1,2</sup> C. Y. Zheng,<sup>1,2</sup> and X. T. He<sup>1,2</sup><sup>1</sup>*Center for Applied Physics and Technology, HEDPS, and State Key Laboratory of Nuclear Physics and Technology, School of Physics, Peking University, Beijing 100871, People's Republic of China*<sup>2</sup>*Institute of Applied Physics and Computational Mathematics, Beijing 100088, People's Republic of China*

(Received 16 August 2021; revised 8 December 2021; accepted 10 February 2022; published 22 February 2022)

In one-dimensional particle-in-cell simulations of a plasma irradiated by linearly polarized lasers from both sides of boundaries, it is found that there is an appreciable growth of the electromagnetic field in cavitons in the transverse direction perpendicular to the direction of polarization, which indicates the polarization conversion of the electromagnetic field in cavitons. This paper demonstrates the mechanism of this phenomenon based on parametric resonance induced by ponderomotive force with twice the frequency of the electromagnetic radiation in the caviton. We develop a theoretical model and verify it with simulation results. This phenomenon contributes to the heating and acceleration of particles and traps more EM energy in cavitons.

DOI: [10.1103/PhysRevE.105.L023202](https://doi.org/10.1103/PhysRevE.105.L023202)

In laser-plasma interactions, stable and long-living structures with depressed densities named cavitons, also named relativistic electromagnetic solitons, can be formed in plasmas irradiated by intense lasers. They can trap solitonlike electromagnetic (EM) radiation whose frequency is lower and amplitude is larger than the laser. Cavitons remain or drift with a small velocity in uniform plasma, inside which the profiles of electric field are half-cycle structures, while the profiles of magnetic field are cycle structures. A large percent of laser pulse energy is contained in cavitons after they are formed in a plasma.

Cavitons have been investigated in many studies by simulations. In one-dimensional (1D) configuration, cavitons can be formed in plasmas with low electron density (less than  $0.3n_c$ ,  $n_c$  being the critical density for the incident laser light) [1–5] and high electron density (approaching or exceeding  $n_c$ ) [6–8]. Cavitons have also been found to exist in two- (2D) and three-dimensional (3D) configurations [8–13]. Generally, the mechanism of the formation of cavitons is related to amplified stimulated Brillouin scattering (SBS) light [1] or the action of plasma gratings [4,7] undergoing Raman-type instability. After formation, electrons are heated and accelerated by the breaking of Langmuir waves in the density gradients of cavitons [6], while ions by Coulomb explosion [10,11]. Cavitons play an important role in describing the nonlinear behavior of plasmas, such as the acceleration of electrons resulting in the saturation of SBS [14], and synchrotron radiation in 3D circularly polarized incident light configuration [12]. They can affect many applications, such as inertial confinement fusion and particle acceleration.

The theoretical study of cavitons induced by linearly polarized [13,15–17] or circularly polarized [18–21] light has been investigated in several studies for cold or warm plasmas. The cavitons induced by linearly polarized light are different from

those induced by circularly polarized light for its oscillatory vector potential, which can lead to parametric resonance, and explain our novel discovery in the simulations that the EM fields perpendicular to the direction of polarization in cavitons grow exponentially. Parametric resonance occurs when the external force acts on the oscillation system, which can be attributed to the periodic variation of parameters with time. The resonance is the most violent when the parameter frequency is close to twice the characteristic frequency [22]. Consequently, the polarization property is converted, which affects the property of the trapped field, and thereby the heating and acceleration of particles.

In this paper, we use one-dimensional particle-in-cell (1D-PIC) code EPOCH to simulate the formation of cavitons. The laser propagates in the  $x$  direction, the incident laser is linearly polarized in the  $y$  direction, and the  $z$  direction is perpendicular to both of them. The linearly polarized lasers are injected from both sides of boundaries, whose intensities are both  $I\lambda_0^2 = 3.4 \times 10^{15} \text{ W } \mu\text{m}^2/\text{cm}^2$ , i.e.,  $eE_y/m_e\omega_0c = 0.05$ , where  $\lambda_0$ ,  $\omega_0$ , and  $E_y$  are the wavelength, angular frequency, and the electric field of the incident lights, respectively. The total simulation length is  $1000k_0^{-1}$ , where  $k_0 = 2\pi/\lambda_0$  is the wave number in vacuum. The initial plasma is located at the center of the simulation box with the length of  $700k_0^{-1}$ . The electrons to ions mass ratio  $m_e/m_i$  is  $1/1836$  and the charge of ions  $Z$  is 1. The initial velocity distribution functions are Maxwellian with temperature of electrons  $T_e = 1 \text{ keV}$  and ions  $T_i = 0.5 \text{ keV}$ , respectively. The space is discretized into a grid with 30 000 points, i.e., the mesh size  $\Delta x = 1/30 k_0^{-1}$ . The number of particles per cell is 300. The boundaries of particles are open.

The number of cavitons is related to the difficulty of their generation. In order to generate as many cavitons as possible for observation, parameters of the plasma and lasers should be set properly. Preliminary simulations yield that cavitons have a higher chance of generation when the electron density is near the critical density for nonrelativistic laser intensity, and

\*liuzj@iapcm.ac.cn

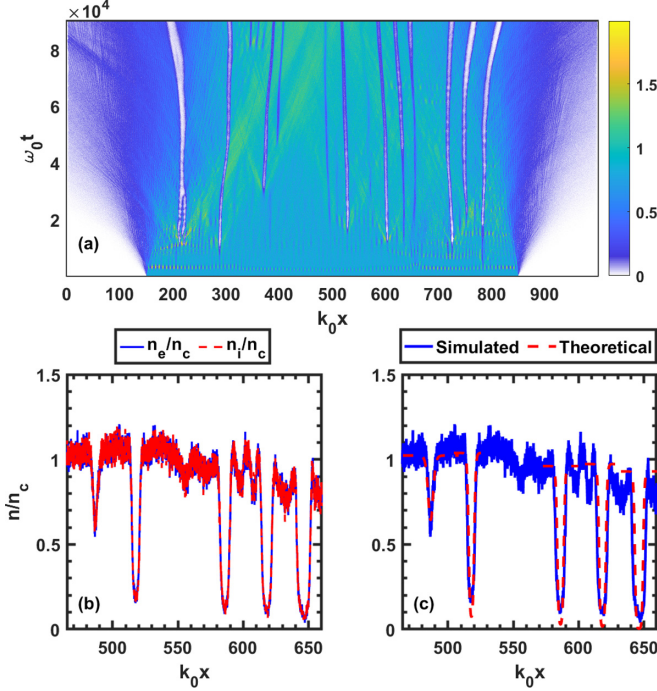


FIG. 1. (a) The evolution of electron density  $n_e/n_c$ , cavitons almost have no drift velocity except a few cavitons near the boundaries. (b) The density profiles of electrons (blue solid line) and ions (red dashed line), the almost coincidence of the curves implies that cavitons in the simulation are quasineutral. (c) Comparison of the density profile of electrons between the simulation results (blue solid line) and the analytical results (red dashed lines). Shallower cavitons have lower frequencies.

continuous laser irradiation also contributes. Thus, the initial density of electrons and ions are both  $0.8n_c$  homogeneously, and the lasers irradiate the plasma continually in the simulation time.

The evolution of electron density  $n_e/n_c$  is shown in Fig. 1(a). Several cavitons are formed after the formation of plasma gratings, and then they remain relatively stable and long living. The density profiles of electrons of some cavitons at  $t = 90\,000 \omega_0^{-1}$  are shown in Fig. 1(b). The cavitons are quasineutral and almost have no drift velocity except a few cavitons near the boundaries, which is consistent with the fact that cavitons move with acceleration against the density gradient [23]. We mainly focus on the nondrifted and quasineutral cavitons in warm plasmas irradiated by circularly polarized incident lights [19]. Then we modify it to the case of nonrelativistic, linearly polarized incident lights and neglect the motion of ions for  $m_e/m_i \ll 1$ . The solutions can be obtained by solving the following equations,

$$\frac{\partial^2 a_X}{\partial x^2} + \omega^2 a_X = a_X e^{-\frac{a_X^2}{4\lambda_e}} e^{\frac{\varphi}{\lambda_e}}, \quad (1)$$

$$\varphi = \left( \frac{1}{\lambda_e} + \frac{Z}{\lambda_i} \right)^{-1} \frac{a_X^2}{4\lambda_e}, \quad (2)$$

$$n_e(x) = N_e e^{-\frac{1}{\lambda_e} \left( \frac{a_X^2}{4} - \varphi \right)}, \quad (3)$$

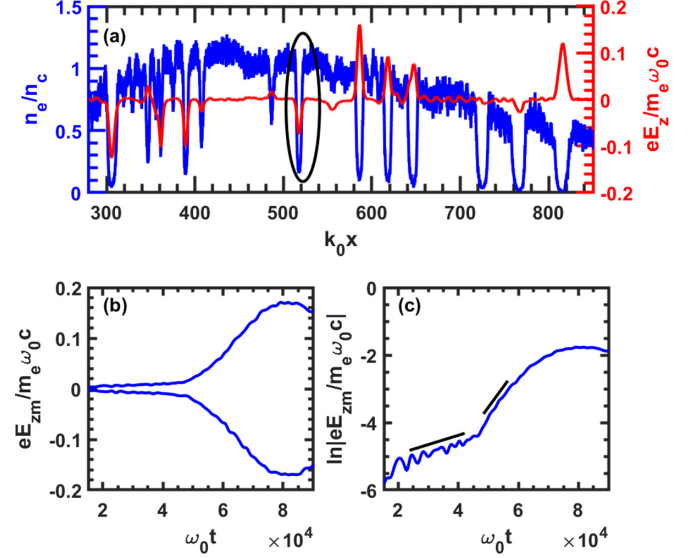


FIG. 2. (a) The snapshot of  $E_z$  and  $n_e$  at  $t = 90\,000 \omega_0^{-1}$ . There is a prominent  $E_z$  in each caviton. Note that it exists in every caviton. Some small values are just caused by the small instantaneous value at this moment. (b) The curve of  $E_{zm}$  vs  $t$  in the circled caviton in (a), where  $E_{zm}$  is the envelope of  $E_z$ . This caviton is formed after around  $t \approx 15\,000 \omega_0^{-1}$ . (c) The curve of logarithm of the (upper) envelope of  $E_z$  vs  $t$  in the caviton. There are two distinct growth rates marked with black straight lines in the figure. It eventually saturates when  $E_z$  grows to be nearly as large as  $E_y$ .

where  $a_X(x) = eA_X(x)/m_e c$  and  $A_X(x)$  is the spacial component of the vector potential  $A(x, t) = A_X(x) \cos \omega t$ ,  $\lambda_{e,i} = T_{e,i}/m_e c^2$ , and  $\varphi = e\phi/m_e c^2$ . Moreover,  $N_e$  is unperturbed electron density, which is also the density on both sides of the caviton. The equations have been reduced to the nonrelativistic limit, and there is an additional factor of  $1/2$  on  $a_X^2$ , which represents the average effect of linearly polarized light. The red dashed lines in Fig. 1(c) represent the numerical results of the modified theoretical solutions, where the simulation results and the numerical solutions are similar, and the influence of the discrepancy is discussed later.

Figure 2(a) shows that, at the end of the simulation time ( $t = 90\,000 \omega_0^{-1}$ ), there is obvious large  $E_z$  in every caviton, though the incident lights are polarized in the  $y$  direction. Figure 2(b) shows the process of the growth of  $E_z$  in one caviton located at  $x \approx 530 k_0^{-1}$ , and the growth is approximately exponential [see Fig. 2(c)]. Another simulation shows that, if there is no thermal motion in  $z$  direction, the initial fluctuating  $E_z$  is zero and  $E_z$  remains zero in the simulation. It is conjectured that there is an instability of  $E_z$  in the caviton. The explanation can be given via the principle of parametric resonance as follows.

Unlike the case in which incident light is circularly polarized, the magnitude of vector potential  $A$  of the linearly polarized light is oscillatory with frequency  $\omega$ . The ponderomotive force is proportional to  $A^2$ , resulting in a component of  $2\omega$  frequency. It drives the longitudinal velocity with  $2\omega$ , and thereby the frequency of density and current density also have a component of  $2\omega$ . Hence,  $A$  satisfies an equation of

parametric resonant, which leads to the exponential growth of  $A_z$ . Then  $E_z$  also grows exponentially for  $E_z = -\partial A_z/\partial t$ .

The hydrodynamic equations for electrons are given by

$$\frac{\partial n_s}{\partial t} + \frac{\partial(n_s v_s)}{\partial x} = 0, \quad (4)$$

$$\frac{\partial v_s}{\partial t} = -\frac{q_s}{m_s} \frac{\partial \phi}{\partial x} - \frac{\gamma_s T_s}{n_s m_s} \frac{\partial n_s}{\partial x} - \frac{1}{2} \frac{\partial}{\partial x} \left( \mathbf{v}_s - \frac{q_s \mathbf{A}}{m_s} \right)^2, \quad (5)$$

where  $n_s$ ,  $v_s$ ,  $q_s$ ,  $m_s$ ,  $\gamma_s$ , and  $T_s$  are the density, longitudinal velocity, charge, mass, adiabatic index, and temperature of  $s$ th species ( $s = e, i$  for electrons or ions), respectively. We can assume that  $n_e = n_{e0} + n_{e1} \cos 2\omega t$ ,  $n_{e0} = n_{i0}$  for quasineutral approximation,  $m_e \ll m_i$ , and  $n_{i1} \ll n_{e1}$  for the slow response of ions, and then the equations of scalar and vector potentials are given by

$$\frac{\partial^2 \phi}{\partial x^2} = \frac{e}{\epsilon_0} n_{e1} \cos 2\omega t, \quad (6)$$

$$\frac{\partial^2 \mathbf{A}}{\partial x^2} - \frac{1}{c^2} \frac{\partial^2 \mathbf{A}}{\partial t^2} = \frac{\omega_{pe}^2 n_e}{N_e} \mathbf{A}, \quad (7)$$

where  $\omega_{pe} = \sqrt{N_e e^2 / \epsilon_0 m_e}$  is the electron plasma frequency.

The growth rate of the field in the whole caviton can be represented by the growth rate at its central point, where  $\partial n_e / \partial x = 0$  is satisfied by virtue of its bilateral symmetry. The combination of Eqs. (4), (5), and (6) gives

$$4\omega^2 n_{e1} \cos 2\omega t = \frac{e^2 n_e}{m_e \epsilon_0} n_{e1} \cos 2\omega t - \frac{\gamma_e T_e}{m_e} \frac{\partial^2 n_e}{\partial x^2} - \frac{e^2}{m_e^2} \frac{\partial}{\partial x} \left( n_e A \frac{\partial A}{\partial x} \right). \quad (8)$$

When  $A_z \ll A_y$  at the onset of the formation of cavitons, the vector potential can be decomposed as  $A(x, t) \approx A_y(x, t) = A_X(x)A_T(t)$ , where  $A_X(x)$  and  $A_T(t)$  are the spatial and temporal components of  $A(x, t)$  or  $A_y(x, t)$ . The amplitude of  $A_y$  is basically unchanged, and thus the temporal component can be regarded as  $A_T(t) = \cos \omega t$ . Then  $\partial A_X / \partial x = 0$  is satisfied at central point and

$$\frac{\partial^2 A_X}{\partial x^2} + \frac{\omega^2}{c^2} A_X = \frac{\omega_{pe}^2 n_e}{N_e} A_X. \quad (9)$$

Comparing the coefficients of  $\cos 2\omega t$  terms in Eq. (8) gives

$$4\omega^2 n_{e1} = \frac{e^2 n_e}{m_e \epsilon_0} n_{e1} - \frac{e^2 n_e}{2m_e^2} \frac{\partial}{\partial x} \left( A_X \frac{\partial A_X}{\partial x} \right). \quad (10)$$

By substituting  $n_e/N_e \rightarrow n_e$ ,  $\omega_{pe} t \rightarrow t$ ,  $\omega_{pe} x/c \rightarrow x$ , and  $a = eA/m_e c$  to make normalizations,  $n_{e1}$  can be obtained as

$$n_{e1} = \frac{1}{2} \left( \frac{\omega^2 - n_b}{4\omega^2 - n_b} \right) n_b a_m^2, \quad (11)$$

where  $n_b$  and  $a_m$  are the central values of  $n_e$  and  $eA_X/m_e c$ , respectively.

Next we consider the equation of the vector potential in the  $z$  direction

$$\frac{\partial^2 a_z}{\partial x^2} - \frac{\partial^2 a_z}{\partial t^2} = n_e a_z, \quad (12)$$

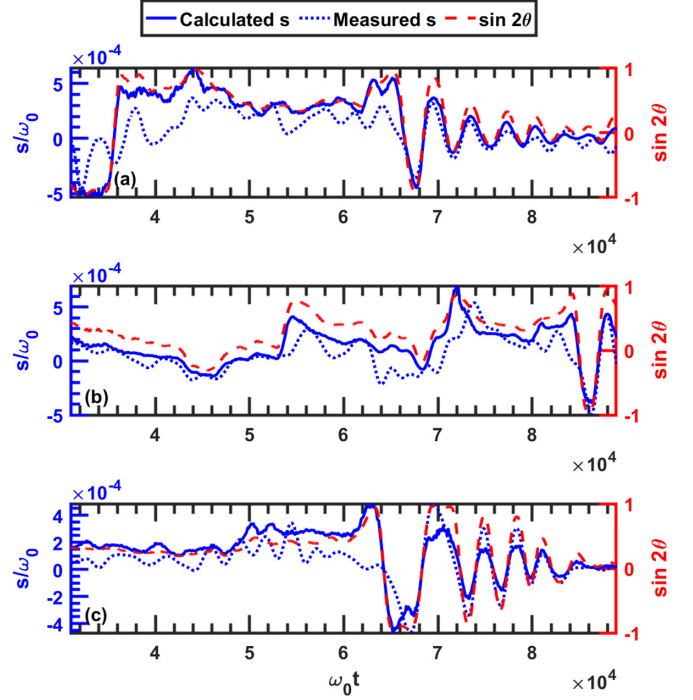


FIG. 3. The time dependence of the values of the growth rates on the right-hand (blue solid lines) and left-hand (blue dotted lines) sides of Eq. (16) in three simulated cavitons. Additionally, it also shows the time dependence of  $\sin 2\theta$  (red dotted line) and its consistency with the growth rate.

which is decomposed as  $a_z(x, t) = a_{zX}(x)a_{zT}(t)$ , and we assume that

$$\frac{\partial^2 a_{zX}}{\partial x^2} = -\omega^2 a_{zX} + (n_{e0} + \Delta n) a_{zX}, \quad (13)$$

$$\frac{\partial^2 a_{zT}}{\partial t^2} + (\omega^2 + \Delta n + n_{e1} \cos 2\omega t) a_{zT} = 0, \quad (14)$$

where we have supplemented an additional density discrepancy  $\Delta n \ll n_{e0}$ , which is necessary as discussed below. Equation (14) is a Mathieu differential equation. Searching a solution in the format of

$$a_{zT} = \alpha(t) \cos(\omega t + \theta), \quad (15)$$

where  $\alpha(t) \sim e^{st}$ ,  $\theta$  is the phase difference between  $A_y$  and  $A_z$ , and  $s$  is the growth rate and satisfies  $s \ll \omega$ , we can obtain

$$s = \frac{n_{e1}}{4\omega} \sin 2\theta = \frac{1}{8\omega} \left( \frac{\omega^2 - n_b}{4\omega^2 - n_b} \right) n_b a_m^2 \sin 2\theta \quad (16)$$

and

$$\Delta n = -\frac{n_{e1}}{2} \cos 2\theta. \quad (17)$$

The parameters in Eq. (16),  $s$ ,  $\omega$ ,  $n_b$ ,  $a_m$ , and  $\theta$ , can all be measured from the simulation results, which reveals that there is an interconnection among them. Figure 3 demonstrates the time dependence of three growth rates in their respective cavitons, where the blue solid lines represent the growth rates calculated on the right-hand side of Eq. (16), while the blue dotted lines represent the growth rates obtained by directly measuring the slope of the envelope of  $\ln |E_z|$ . The two are in

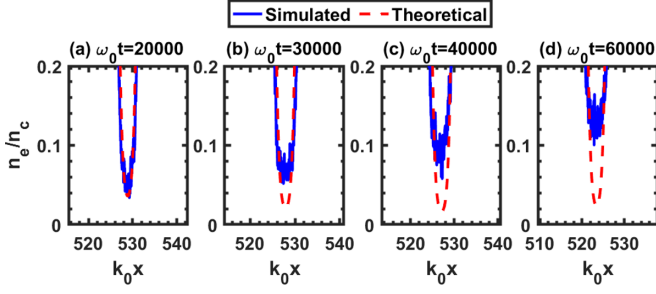


FIG. 4. Comparison of the density of electrons at the bottom of the same caviton from the simulation results and that obtained from Eqs. (1)–(3). The discrepancy becomes larger with time due to the increase of temperature.

great agreement, especially because when there is a significant variation in one of the growth rate, the variation of the other is usually synchronized. The validity of Eq. (16) is a strong evidence that parametric resonance causes the growth of  $E_z$ . Figure 3 also demonstrates the time dependence of  $\sin 2\theta$ , where the variations of  $\sin 2\theta$  and growth rate are consistent. Other parameters,  $\omega$ ,  $n_b$ , and  $a_m$ , vary slowly in time. It indicates that the value of  $\sin 2\theta$  has a major influence on the time dependence of  $s$ .

The phase difference  $\theta$  is relevant to the density discrepancy  $\Delta n$  according to Eq. (17). We can speculate that the variation of growth rate is affected by the phase difference and ultimately by the disturbance of density. In addition to the disturbance caused by the inherent property of particle-in-cell (PIC) simulation, the deformation of cavitons caused by particle heating and acceleration is another important factor. Simulation yields that Eq. (1) predicts relatively accurate  $a_m$ , but the  $n_b$  predicted by Eq. (3) is less than that obtained from the simulation results. As shown in Fig. 4, the discrepancy between  $n_e$  (and  $n_b$ ) obtained by simulation and theory becomes larger in time. As a result, the sign of  $s$  changes after around  $t = 60\,000\omega_0^{-1}$ , which may be a mechanism of saturation.

The specific location and time of the generation of cavitons are somewhat random and sensitive to the initial conditions. Therefore, it is elusive to predict the parameters in cavitons precisely when only the initial parameters of laser and plasma are provided. Instead, it is possible to roughly estimate the maximum value of growth. By using  $(\omega^2 - n_b)/(4\omega^2 - n_b) < 1/4$  and Eq. (3), Eq. (16) can be rewritten as

$$s < \frac{1}{32\omega} e^{-\frac{C a_m^2}{2}} a_m^2, \quad (18)$$

where  $C = Z/2(\lambda_i + Z\lambda_e) \approx 1/2\lambda_e$ . By integrating Eq. (1), one can obtain  $\int_0^{a_m} a \exp(-Ca^2/2) da = \omega^2 a_m^2$ , i.e.,  $\omega^2 = [1 - \exp(-Ca_m^2/2)]/Ca_m^2$ . The maximum value of  $s$  then can be roughly expressed as  $s_{\max} \approx 0.1182 \lambda_e^{3/4}$ , which shows that the order of magnitude of  $s_{\max}$  is in the range of  $10^{-5} \omega_{pe}$  to  $10^{-3} \omega_{pe}$  when the temperature of electron is in the range of 10 eV to 1.5 keV. Generally, the simulated growth rate is smaller than  $s_{\max}$ , but in the same order of magnitude.

This unstable growth is found to be general, since parametric resonance induced by  $2\omega$  ponderomotive force exists

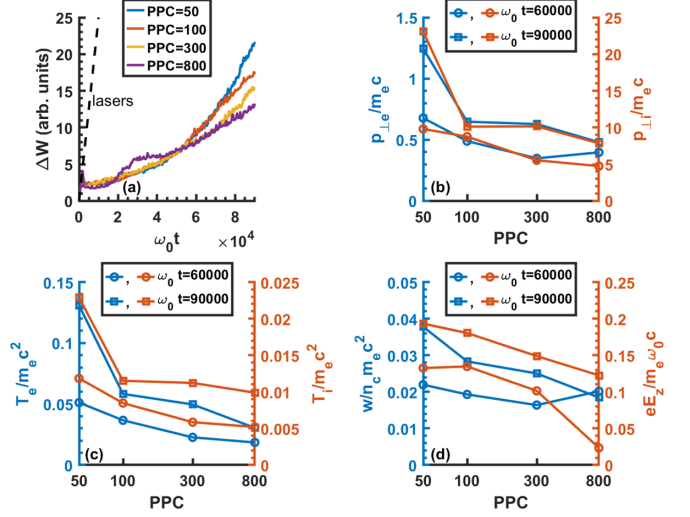


FIG. 5. (a) Time dependence of the total energy increment  $\Delta W$  of plasma for different PPCs. The black dashed line indicates the energy emitted by lasers. (b) Transverse momentum, (c) temperature of electrons and ions, and (d) EM energy density for different PPCs.  $E_z$  is also plotted in panel (d) to ensure that a larger PPC indicates a smaller initial noise level and a smaller impact of parametric resonance. All of these values are obtained by calculating the averages of the top five peaks to reduce random errors.

in different kinds of cavitons. Cavitons can also generate in low-density plasmas where the EM fields often possess multipole structures [20] and electron-positron plasmas where the thermal energy of particles is extremely high [24]. Under these circumstances, the growth can still be observed from simulations.

To further explore the impact of this phenomenon, for different initial noise levels, we calculate the total energy increment  $\Delta W$  of plasma obtained by integrating the Poynting vector with respect to time and summing at both boundaries. In PIC simulation, the initial noise level can be adjusted by changing the number of particles per cell (PPC). The initial noise level becomes larger when PPC becomes smaller. The time dependence of  $\Delta W$  is shown in Fig. 5(a). After approximately  $t = 60\,000\omega_0^{-1}$ ,  $\Delta W$  becomes larger when PPC becomes smaller. Hence, parametric resonance makes more energy contained in the plasma. Since  $\Delta W$  comprises kinetic energy, thermal energy, and EM energy, we calculate the transverse momentum of electrons  $p_{\perp e}$  and ions  $p_{\perp i}$ , the temperature of electrons  $T_e$  and ions  $T_i$ , and the EM energy density  $w$  in cavitons for different PPCs at  $t = 60\,000\omega_0^{-1}$  and  $t = 90\,000\omega_0^{-1}$ , which are shown in Figs. 5(b)–5(d), respectively. Though there may be random errors caused by the unpredictability of cavitons, it can still be clearly seen that parametric resonance contributes to the heating and acceleration of particles and traps more EM energy in cavitons.

In conclusion, we have shown and explained the polarization conversion caused by instability of  $E_z$ . We develop a theoretical model which gives the relation between the growth rate and other parameters. The consistence of the simulation result and the model confirms the correctness. The order of magnitude of the growth rate is also estimated. We have

also shown that this phenomenon contributes to the heating and acceleration of particles and makes more EM energy trapped in cavitons. One can enhance or inhibit this phenomenon artificially according to demand. Other impacts and applications of parametric resonance in cavitons could be the subject of future research when the direction of polarization affects physical phenomena. For example, when a relativistic intensity laser irradiates a plasma, cavitons generated by

$s$ - and  $p$ -polarized lasers have different structures [9], or when an external magnetic field is applied to the plasma, the dispersion relation of EM wave is related to its direction of polarization.

This work is supported by the National Natural Science Foundation of China (Grants No. 11875091 and No. 11975059).

- 
- [1] S. Weber, M. Lontano, M. Passoni, C. Riconda, and V. T. Tikhonchuk, *Phys. Plasmas* **12**, 112107 (2005).
- [2] M. Lontano, M. Passoni, C. Riconda, V. T. Tikhonchuk, and S. Weber, *Laser Part. Beams* **24**, 125 (2006).
- [3] B. Li, S. Ishiguro, M. M. Skorić, and T. Sato, *Phys. Plasmas* **13**, 042303 (2006).
- [4] S. X. Luan, Q. J. Zhang, and Z. M. Sheng, *Appl. Phys. B* **93**, 793 (2008).
- [5] C. Z. Xiao, Z. J. Liu, D. Wu, C. Y. Zheng, and X. T. He, *Phys. Plasmas* **22**, 052121 (2015).
- [6] N. J. Sircombe, T. D. Arber, and R. O. Dendy, *Phys. Plasmas* **12**, 012303 (2005).
- [7] Z. J. Liu, X. T. He, C. Y. Zheng, and Y. G. Wang, *Phys. Plasmas* **16**, 093108 (2009).
- [8] D. Wu, W. Yu, S. Fritzsche, C. Y. Zheng, and X. T. He, *Phys. Plasmas* **26**, 063107 (2019).
- [9] S. V. Bulanov, T. Z. Esirkepov, N. M. Naumova, F. Pegoraro, and V. A. Vshivkov, *Phys. Rev. Lett.* **82**, 3440 (1999).
- [10] N. M. Naumova, S. V. Bulanov, T. Z. Esirkepov, D. Farina, K. Nishihara, F. Pegoraro, H. Ruhl, and A. S. Sakharov, *Phys. Rev. Lett.* **87**, 185004 (2001).
- [11] T. Esirkepov, K. Nishihara, S. V. Bulanov, and F. Pegoraro, *Phys. Rev. Lett.* **89**, 275002 (2002).
- [12] T. Esirkepov, S. V. Bulanov, K. Nishihara, and T. Tajima, *Phys. Rev. Lett.* **92**, 255001 (2004).
- [13] G. Sánchez-Arriaga and E. Lefebvre, *Phys. Rev. E* **84**, 036403 (2011).
- [14] S. Weber, C. Riconda, and V. T. Tikhonchuk, *Phys. Plasmas* **12**, 043101 (2005).
- [15] L. Hadžievski, M. S. Jovanović, M. M. Škorić, and K. Mima, *Phys. Plasmas* **9**, 2569 (2002).
- [16] G. Lehmann, E. W. Laedke, and K. H. Spatschek, *Phys. Plasmas* **13**, 092302 (2006).
- [17] C. S. Liu, V. K. Tripathi, and B. Eliasson, *High-Power Laser-Plasma Interaction* (Cambridge University Press, Cambridge, UK, 2019), Chap. 4.
- [18] V. A. Kozlov, A. G. Litvak, and E. V. Suvorov, *Zh. Eksp. Teor. Fiz.* **76**, 148 (1979) [*Sov. Phys. JETP* **49**, 75 (1979)].
- [19] M. Lontano, M. Passoni, and S. V. Bulanov, *Phys. Plasmas* **10**, 639 (2003).
- [20] V. Saxena, A. Das, A. Sen, and P. Kaw, *Phys. Plasmas* **13**, 032309 (2006).
- [21] K. Yamanouchi, S. L. Chin, P. Agostini, and G. Ferrante, *Progress in Ultrafast Intense Laser Science II* (Springer Science & Business Media, Berlin, 2007).
- [22] L. D. Landau and E. M. Lifshitz, *Mechanics*, Course of Theoretical Physics Vol. 1 (Elsevier, Oxford, UK, 1976), pp. 80–84.
- [23] Y. Sentoku, T. Zh. Esirkepov, K. Mima, K. Nishihara, F. Califano, F. Pegoraro, H. Sakagami, Y. Kitagawa, N. M. Naumova, and S. V. Bulanov, *Phys. Rev. Lett.* **83**, 3434 (1999).
- [24] M. Lontano, S. Bulanov, and J. Koga, *Phys. Plasmas* **8**, 5113 (2001).